DOI: 10.13009/EUCASS2017-213

Supersonic Wind Tunnel Tests of a Standard Model at High Angles of Attack

Dijana Damljanović and Djordje Vuković**
** Military Technical Institute (VTI)*
Ratka Resanovića 1, 11030 Belgrade, Serbia

Abstract

Following the requirements for supersonic wind tunnel tests at high angles of attack, the capability to verify the high-angle-of-attack provisions in the T-38 wind tunnel of VTI was needed. Such task is conveniently performed by tests of a standard model. As the volume of reference data on standard models at high angles of attack was small, a series of tests of the HB-2 model at Mach numbers 1.5 to 4 and angles of attack up to 30° was performed to create a reference database for future tests. Results were successfully correlated to lower-angle-of-attack data from other facilities.

1. Introduction

Requirement for high-speed wind tunnel testing at high angles of attack (high-AoA) has existed for decades [1]-[3]. This capability was necessary for testing of atmospheric re-entry of manned capsules during the early spaceflight programs, as well as in the development of the Space Shuttle Orbiter, which, for example, started its atmospheric reentry at Mach 25 and angle of attack of about 40º, the angle of attack dropping below 20° only below Mach 4 [4][5]. Moreover, modern missiles often manoeuvre at supersonic high-AoA conditions, requiring, during the development, appropriate experimental verification of their aerodynamic characteristics. Recent development of many concepts of reusable launch vehicles with fly-back capabilities also underscores the continued need for high-angle-of-attack wind tunnel testing at supersonic speeds. A considerable amount of theoretical and experimental work has been dedicated to high-AoA aerodynamics [5]-[8]. Also, engineering-level prediction codes were extended to encompass high-AoA conditions [9].

Another realm in which the need for high-AoA supersonic wind tunnel tests is expressed is the computational fluid dynamics (CFD). A number of codes dealing with the high-AoA aerodynamics is being developed, mostly tuned to support the development of spaceplanes, reentry capsules and similar vehicles. The developers admit that high-AoA aerodynamics presents many challenges [10]-[12]. Experimental data to be used as test cases for these codes would be welcome.

On the other hand, execution of high-AoA wind tunnel tests may be complicated by a number of factors. Because of the constraints of the wind tunnel structures, the dimensions of the test sections and the placements of the model support mechanisms, the "basic" model supports of many high-speed wind tunnels permit movements of the model only in the relatively small range of angles of attack, usually ±15º to ±20°. In order to perform high-AoA tests, additional provisions in the form of bent stings, twin-roll mechanisms, etc. that shift the AoA range to higher positive values are usually strapped onto the "basic" model supports. However, such add-ons may complicate testing because of the increased aerodynamic blockage in the rear of the wind tunnel test section, interference by shock waves generated by the added parts of the model support, increased operating pressure, increased model-support deflections and lowered natural frequencies of the model-support assemblies. In such cases it is good to verify the complete wind tunnel measurement chain by testing of a standard model.

Unfortunately, the database of reference test results of standard models at high-AoA in the supersonic speed range is relatively small. Military Technical Institute (VTI) in Belgrade, Serbia, was faced with this problem in the preparations of some recent high-AoA tests in its T-38 trisonic wind tunnel [13][14]. VTI follows the practice of confirming the validity of its wind-tunnel measurement systems by periodic testing of AGARD-B standard models, as well as by performing brief standard-model test campaigns before some tests with specific requirements,[15][16]. As AGARD-B was not convenient for Mach numbers above 2 because of the high dynamic pressure in the T-38

DOI: 10.13009/EUCASS2017-213

wind tunnel and high supersonic starting loads [17][18], the supersonic-hypersonic configuration known as HB-2 [19] was selected as an additional standard model for high Mach number tests. An overview of available reference data [19]-[26] for the HB-2 model showed that the tests in various wind tunnels were mostly limited to angles of attack not larger than 15°, except for a small number of Mach 10 tests [24] in a JAXA wind tunnel at AoA up to 30º. Therefore, as there were no reference data available, it was decided to create VTI's own standard-model reference database for future supersonic high-AoA testing. To this end, a short series of tests of HB-2 models was performed at Mach numbers 1.5 to 4 at AoA up to 30°. Two sizes of the HB-2 model were tested, having 75 mm and 100 mm body diameters, on two internal wind tunnel balances. An articulated bent sting, set to 10º bend angle was used as the model support, shifting the AoA range of the T-38 wind tunnel model support from the standard −12°/+20° to −2°/+30°. Obtained data was compared to results [27] of previous tests performed in the same wind tunnel in the lower AoA range, and with test results [19]-[21] from the wind tunnels of AEDC and ONERA and limited free-flight data from NASA Ames Pressurized Ballistic Range [22].

2. The HB correlation model

The initiative for selecting a suitable configuration of a high velocity correlation model was started at the joint meeting of AGARD and STA (Supersonic Tunnel Association) in the year 1959. This resulted in adoption, in 1960, of two hypervelocity ballistic model configurations, designated as HB-1 and HB-2 (Figure 1, [19]), which consisted of a blunt cone-cylinder with a flare added to the HB-2 configuration, the latter shape being included to provide a model that would be less sensitive to viscous effects. The inclusion of the HB model into the AGARD standard models was proposed in 1963.

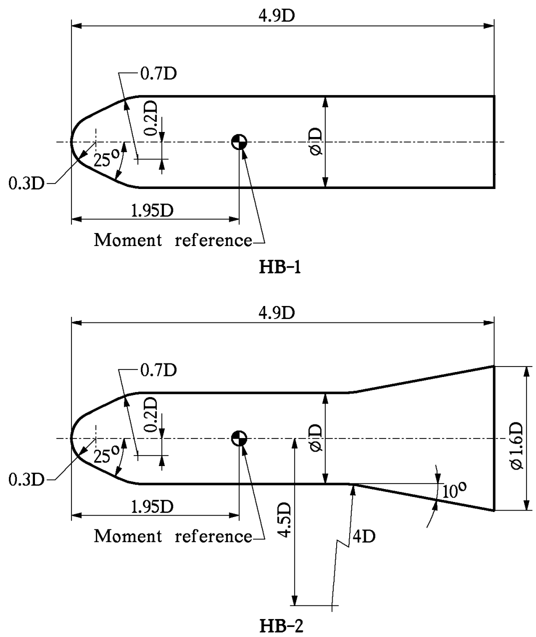

Figure 1: Definition of the HB model configurations, [19]

Both configurations of the model are axisymmetric cone-cylinders with 25º nose cone half-angle, differing by the addition of a 10° tail flare in the HB-2 configuration. The junctures of the nose and flare with the cylinder are smooth radius fairings. The unit length for the definition of model geometry is the diameter D of the cylindrical part of the body. Model length is defined as 4.9D for both configurations. Moments reduction centre is at 1.95D from the nose.

A recommended geometry of the support sting (Figure 2), to be used when testing HB-1 and HB-2 models, was also defined, specifying a constant diameter of no more than 0.3D for a length of at least 3D with a conical windshield of 20° half-angle. The specified maximum diameter and minimum length of the sting were necessary to ensure negligible interference on the base pressure for turbulent flow. It should be noted, however, that the magnitude of aerodynamic loads in high-dynamic-pressure wind tunnels may necessitate the use of stings of larger relative diameters because, even with the best steels available, structural safety of the "standard" sting may be compromised at high angles of attack and high dynamic pressures, as illustrated in Figure 3 [28] whish shows that, at AoA of 30°, dynamic pressure can not exceed approximately 0.15 MPa (1.5 bar) if a safety factor of two is desired for the sting. Large supersonic starting loads in some wind tunnels (VTI T-38 included) reduce the safety factor even further.

DOI: 10.13009/EUCASS2017-213

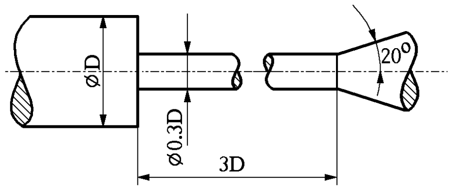

Figure 2: Proposed “standard” sting geometry for the HB models, [19]

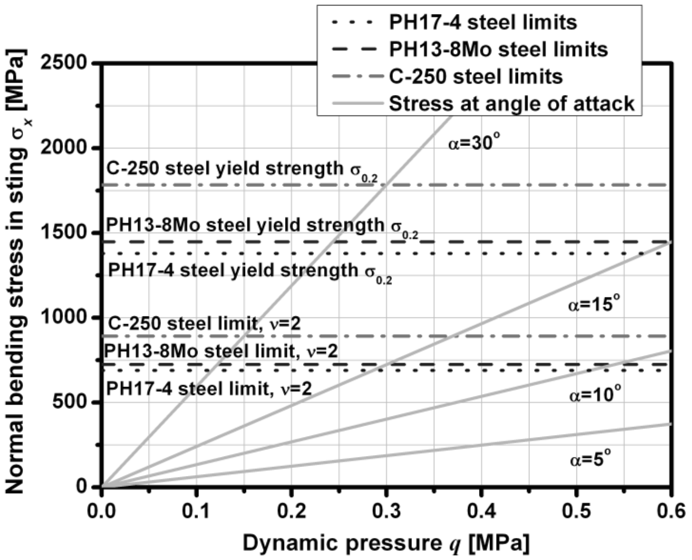

Figure 3: Structural safety limits of a standard HB-2 sting produced from some high-strength steels related to dynamic pressure in wind tunnel test section, [28]

The HB models designed and produced in the VTI workshop for the T-38 wind tunnel were built in two sizes, having 75 mm and 100 mm forebody diameters. The models are intended for measurements of forces and moments, and were designed so that each of them can be tested on at least three different force balances, using suitable adaptors common to both models. Besides, the 100 mm dia. model can be tested on the VTI's dynamic derivatives rig [29], and also, some space in the 100 mm model was provided for future modifications in order to enable measurement of pressure distribution or heat transfer. The models were designed so that they could be quickly assembled and disassembled and consisted of a cylindrical steel core, common to both models, for model-balance mating and an aluminium-alloy outer shell (Figure 4). The design intent was to make the models suitable for use as quick-check standards that can be easily installed in the wind tunnel instead of some currently tested model, should a need for such checkout arise in any future wind tunnel test.

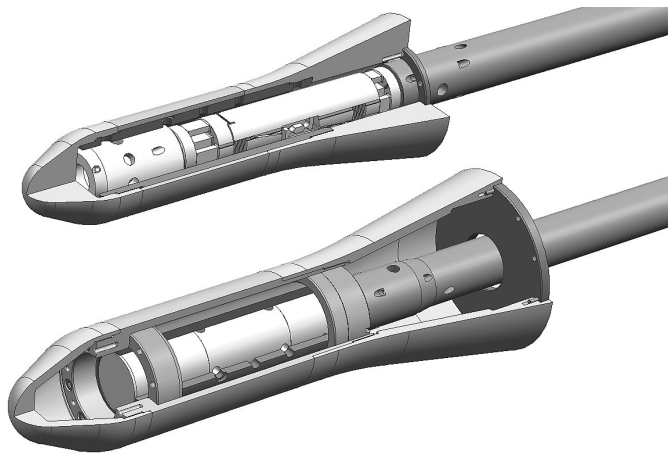

Figure 4: Partial cross-sections (CAD rendering) through the 75 mm dia. and 100 mm dia. HB-2 models produced for the T-38 wind tunnel. Balances and stings are shown

DOI: 10.13009/EUCASS2017-213

3. T-38 wind tunnel test facility

The T-38 test facility at VTI is a blow-down pressurized wind tunnel with a 1.5 m × 1.5 m square test section, Figure 5, [13], Mach number range from 0.2 to 4 and high-Reynolds-numbers capability (up to 110 million per meter). The energy for driving the wind tunnel is stored in five interconnected air tanks with a total volume of 2600 m^3, charged to 20 bar pressure by a 4 MW, 5-stage compressor. During a wind tunnel run, the air from the tanks is released through the wind tunnel and discharged into the atmosphere. Run times vary from 6 seconds to about 90 seconds, depending on test conditions.

For subsonic and supersonic tests, the test section of the T-38 wind tunnel is with solid walls, while for transonic tests, a section with porous walls is inserted in the wind tunnel configuration. Mach number is set and maintained to within 0.5% of the nominal value by means of either a flexile nozzle or by sidewall flaps and/or sidewall blowoff, depending on the test speed range. Stagnation pressure in the test section can be maintained between 1.1 bar and 15 bar, depending on Mach number, and regulated to 0.1% of nominal value.

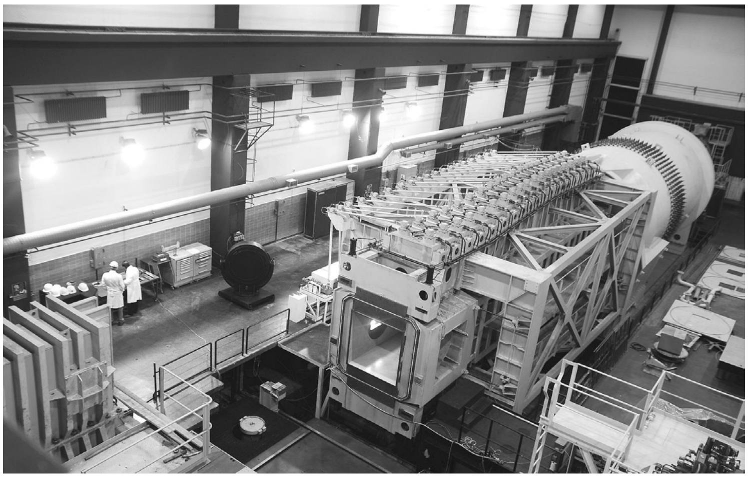

Figure 5: The T-38 trisonic wind-tunnel in VTI, Belgrade

Model is usually supported in the test section by a tail sting mounted on a pitch-and-roll mechanism by which the desired aerodynamic angles can be achieved (Figure 6). Travel range of the pitch-angle mechanism is from −12° to +20° (Figure 7). The −12° limit can be extended to −20° by removing a cover in the rear test section ceiling, but at the seldom-acceptable cost of increased aerodynamic noise, increased minimum operating pressure and increased supersonic starting loads. Travel range of the roll-angle mechanism is 0° to 360°. The facility supports both step-by-step and continuous (sweep) movement of model during measurements.

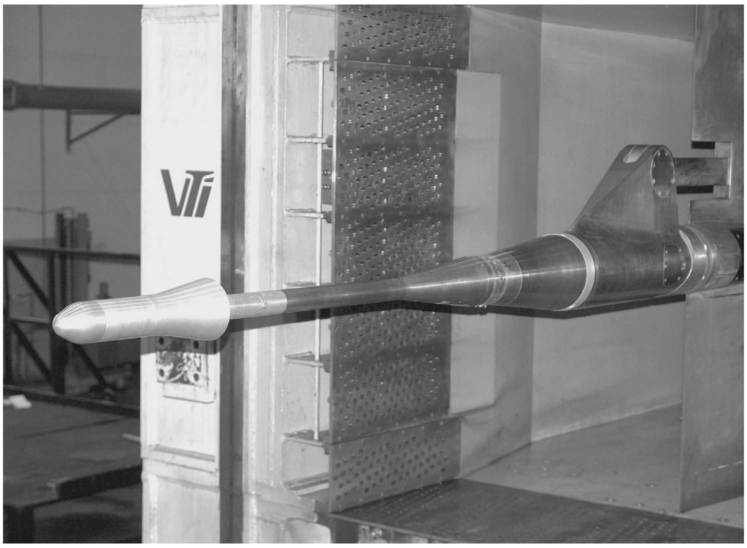

Figure 6: HB-2 model on the straight tail sting in the T-38 wind tunnel of VTI

DOI: 10.13009/EUCASS2017-213

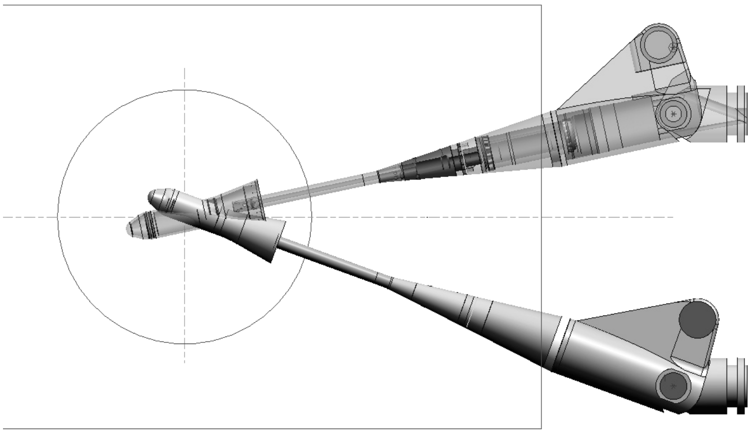

Figure 7: HB-2 model on the standard pitch-and-roll model support mechanism in T-38, showing the minimum and maximum achievable angles of attack

4. Wind tunnel testing in the T-38

4.1 Test matrices

High-AoA tests of the HB-2 model were performed in the Mach number range from 1.5 to 4 and at AoA from −2° to 30º with both models (75 mm and 100 mm forebody dia.), according to the matrix shown in Table 1. The AoA interval was covered in a continuous movement of the model during the measurement (sweep) at 2°/s rate. The smaller model was tested on a lower-load-range six-component balance designated as VTI40B at Mach numbers 1.5 to 2.5 and then again on a higher-load-range six-component balance designated as MkXVIII in the complete Mach 1.5 to 4 range. The larger model was tested on the higher-load-range balance only. Besides, because of the wind tunnel schedule constraints, some Mach numbers were omitted with this model. Stagnation pressure in the test section ranged from 2 bar at Mach 1.5 to 13 bar at Mach 4 and corresponded to dynamic pressures of approximately 0.9 to 1 bar at all Mach numbers. Reynolds number (based on forebody diameter) was in the range from 2.2 millions at Mach 1.5 to 4.5 millions at Mach 4.

Mach numbers for the tests were selected to correspond to those in an earlier test [27] (Figure 6) in T-38 of the 75 mm model in the T-38 wind tunnel on a straight sting and a special high-drag-range balance at AoA up to 15°. Mach numbers 1.5, 2, 3 and 4 also corresponded to those in the tests of the HB-2 models in the Von Karman Facility at AEDC [20], and Mach numbers 1.6, 2.25, 3 and 3.25 corresponded to those in the tests in ONERA S5 Chalias and C4 Vernon wind tunnels [21].

Table 1: Test matrix for the high-AoA HB-2 tests in VTI T-38 wind tunnel

Model size	**Balance**	**Mach number**									
		1.5	**1.6**	**1.8**	**2.0**	**2.25**	**2.5**	**3.0**	**3.25**	**3.5**	**4.0**
75 mm dia.	VTI40B	o	o		o		o				
	MkXVIII	o	o	o	o	o	o	o	o	o	o
100 mm dia.	MkXVIII	o			o	o	o	o			

4.2 Model support

In order to increase the angle-of-attack range for the tests of the HB-2 models, an articulated bent sting was deployed. The sting comprised a conical hub mounted on the roll drive of the standard model support of the wind tunnel, a hinged vertical pylon with a pod for the secondary roll axis, and a straight front part of the sting, on which the internal balances and the models were mounted (Figure 8, Figure 9). When this sting was designed, the shape and size of the conical hub were chosen to be as similar as possible to the front part of the roll-drive of the standard straight-sting model support mechanism (Figure 6, Figure 7), in order to avoid introducing different aerodynamic

DOI: 10.13009/EUCASS2017-213

interference. The cross-sections of the pylon and the secondary roll-axis pod were minimized as well, for the same reason. The pylon could be manually set at different pitch angles in the hub by means of suitably shaped keys, thus producing the desired "bend" angle of the sting in the range of 10° to 20°. For the tests of the HB-2 models, the bend of 10° was selected, thus obtaining an effective AoA range for the model from −2° to +30°. The straight front part of the sting was exchangeable (alternative parts having interfaces for different force balances) and could be manually set at different roll angles at 22.5° increments through a full 360° turn.

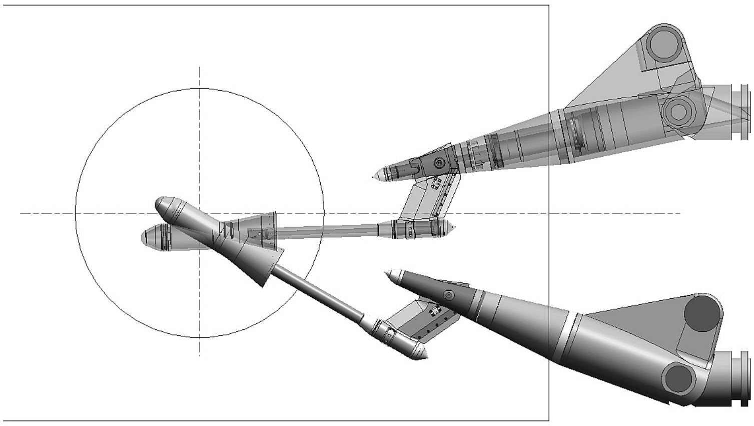

Figure 8: CAD rendering of the 100 mm dia. HB-2 model on the articulated bent sting used in the tests, at extreme angles of attack

Two front parts of the stings were used, with interfaces for the two balances. Both stings had a diameter of 43 mm and were mounted on the hub of the articulated bent sting. The sting-to-model-base diameter ratio was 0.57 for the 75 mm HB-2 model and 0.43 for the 100 mm model. The length of the stings behind model base was more than 3.5 model forebody diameters. However, the recommended sting/base diameter ratio of 0.33 could not be implemented because a sting with a diameter so small would not have been safe in the environment of the T-38 wind tunnel.

a 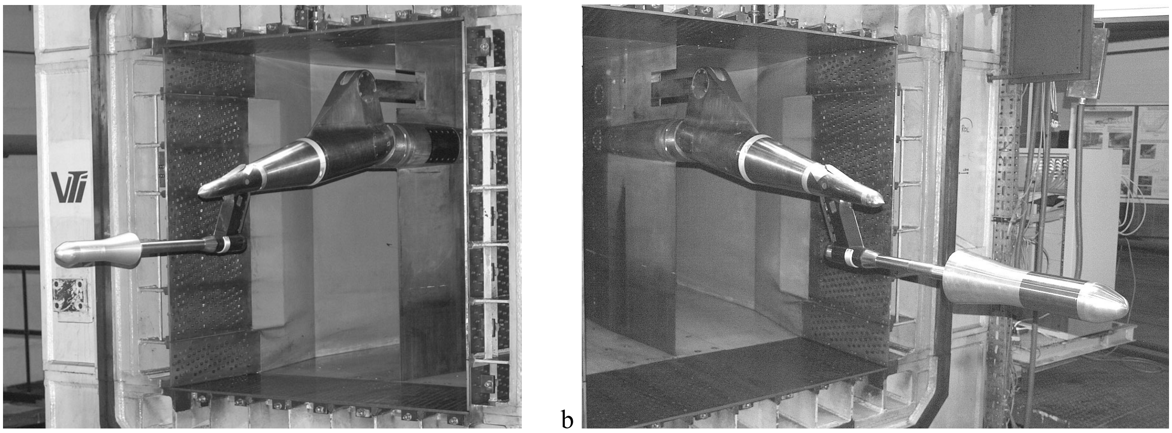 b

Figure 9: Two HB-2 models, with 75 mm diameter (a) and 100 mm diameter (b) on the articulated 10º bent sting in the T-38 wind tunnel.

4.3 Instrumentation, data recording and data reduction

Mach number and dynamic pressure in the test section of the wind tunnel were determined from measurements of two pressures. At Mach numbers 1.5 to 2, those were the stagnation pressure in the settling chamber and the static pressure measured at the sidewall of the test section of the wind tunnel. At Mach numbers above 2, pitot pressure behind a normal shock wave was measured by a probe in the test section instead of the sidewall static pressure, in order to obtain a better accuracy [30] for the computed Mach number and dynamic pressure. High-accuracy (0.01%FS) Mensor CPT6100 absolute-pressure transducers with RS-485 serial digital outputs were used, with the ranges of 17 bar for the stagnation pressure in the settling chamber, 7 bar for the pitot pressure and 3.5 bar for the static pressure. The ranges of the pitot-pressure transducer and the static-pressure transducer were dictated by

DOI: 10.13009/EUCASS2017-213

pressure transients at the start of wind tunnel runs and had to be significantly larger than actually measured pressures: therefore, it was essential to use high-accuracy pressure transducers as the actual measurements were performed in a fraction of their design pressure ranges.

Base pressure on the model was measured by a Druck PDCR42 silicon piezoresistive differential-pressure transducer with 0.35 bar range and measurement uncertainty of 0.05%FS in tests at Mach numbers 1.5 to 2. The active side of this transducer was connected to an orifice on the sting inside the rear side of the model, so that it measured the pressure in the model sting/balance cavity. The model was designed so that this cavity did not have openings towards the outer surface of the model and the measured pressure was assumed to be equal to base pressure. The reference side of the transducer was connected to the tubing leading from the static-pressure port on the sidewall of the test section. At Mach numbers above 2, base pressure was measured by an IHTM SP-1.75A absolute-pressure transducer with 1.75 bar range and 0.05%FS accuracy. The transducers were located on the external side of the model support system and a pneumatic lead was passed from the measurement point on the sting, through the sting and through the model support mechanism to the transducers.

Also, the readings of all pressure transducers were checked at the start of each wind tunnel run by comparison with the reading of a 1.4 bar, RS-485 serial digital-output, Mensor CPT6180 absolute-pressure transducer, similar to the CPT6100 but having higher accuracy (0.01% IS50) and stability, which measured atmospheric pressure.

Stagnation temperature was measured by a custom-made RTD probe comprising an Omega 100W30 thin-film Pt100 element and located in the settling chamber of the wind tunnel. The accuracy of this transducer was approximately ±0.25 K.

The pitching angle of the model support was measured by a Hengstler Acuro AC58 absolute-angle optical encoder with SSI serial digital output, located on the drive spindle of the model support mechanism. The accuracy of reading was typically 0.02°.

All tests of the two HB-2 models were performed at dynamic pressures of about 0.9 to 1 bar, so that, for each model, maximum steady-flow aerodynamic loads were similar throughout the test. However, the models were also subjected to supersonic starting loads [17][18], which occur during the establishment and breakdown of the supersonic flow in the wind tunnel. Those loads are primarily a characteristic of the pressurized blowdown wind tunnels and can exceed several times the steady-state aerodynamic loads. Therefore, they (and not the steady-state loads) are usually relevant for the selection of wind tunnel balances for supersonic tests, and the balances, generally, must have load ranges higher than desired, which can have a negative impact on the accuracy of performed force measurements.

In order to ensure safety against the starting loads, and yet to obtain a good accuracy of the measurement, it was decided to perform the tests of the HB-2 model using two internal balances: one for the smaller 75 mm model at lower Mach numbers, and the other one for the 75 mm model at higher Mach numbers and also for the larger 100 mm Model at all Mach numbers. In order to enable comparison between the results with the two balances, the higher-range balance was also to be used with the 75 mm model at lower Mach numbers.

For the lower-supersonic part of the test (up to Mach 2.5), the selected balance for the 75 mm model was VTI40B, a 40 mm VTI-produced monolithic internal six-component strain gauge device (Figure 10) which was one of the VTI's balances often used for wind tunnel tests of missile-like models. The balance was wired as a direct-read one. Nominal load range of the balance was 3000 N for normal and side forces, 700 N for axial force, 200 Nm for pitching and yawing moment and 50 Nm for rolling moment. As the balance was designed specifically for supersonic tests, it had a significant overload capability (up to 6000 N for normal and side forces), which made it convenient for the test of the HB-2 model where large starting loads were expected. Measurement uncertainty of the balance was better than 0.11%FS for all components but the rolling moment (Table 3).

For the 100 mm model and the upper-supersonic parts of the test with the 75 mm model, the 2-inch Able MkXVIII internal six-component assembled strain gauge balance was selected (Figure 11). It was designed and wired as a force balance, with two components measuring normal forces, two components measuring side forces, one component measuring the axial force and one component measuring the rolling moment. Nominal load range of the balance was 17800 N for the total normal and side forces at zero pitching and yawing moments, 1640 Nm for the total pitching moment at zero normal force, 1360 Nm for the total yawing moment at zero side force, 2700 N for the axial force and 340 Nm for the rolling moment. However, on the basis of expected loads, the balance was calibrated in a "turndown" combined-loads range of 8900 N for normal and side forces, 820 Nm for the pitching moment (simultaneous with the maximum normal force), 680 Nm for the yawing moment (simultaneous with the side force),

DOI: 10.13009/EUCASS2017-213

1800 N for axial force and 170 Nm for rolling moment. As the "turndown" load ranges for transversal forces and moments corresponded to simultaneous loads of approximately 50% of the maximum design loads, the four normal- and side-force measuring elements in the balance were actually calibrated to 100% of their designed load capacity. Measurement uncertainty, from the calibration of the balance, was in the range 0.1-0.17% FS, slightly differing from component to component (Table 3).

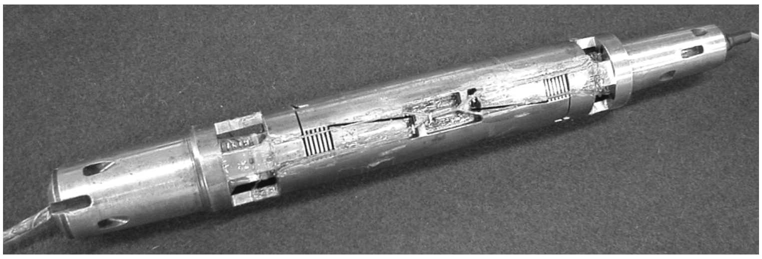

Figure 10: VTI40B 40 mm monolithic balance used in the test.

Figure 11: Able MkXVIII 2-inch assembled balance used in the test.

The data acquisition system consisted of a Teledyne 64-channel "front end" controlled by a personal computer. The data from all analog inputs were digitized by a 16-bit resolution A/D converter in the system with the overall accuracy of about 0.05% of the signals input range. All channels were sampled with the same 300 samples/s rate.

The data from digital input channels, such as the position encoders and pressure transducers of the primary measurement system, were recorded on the parallel-input digital channels of the data acquisition system. As all digital transducers that were used actually produced data in serial formats, pre-processor interfaces based on PIC 16F-series microcontrollers were installed on each digital input channel to convert the received data to parallel format.

The output of a precision IRIG clock was sampled synchronously with other channels, in order to serve as a time base for segmentation of data.

In order to minimize the differences in time lags on various channels during model sweep, the channels for all balance components and base pressure were low-pass filtered to relatively high cut-off frequencies, using 30 Hz 4-pole Butterwort filters. To compensate for the poorer filtering on these channels, these signals were additionally filtered during the data reduction by a 3 Hz non-casual low pass digital filter.

Digitized data were sent through the network to a Compaq Alphaserver DS20E computer and stored on disk for later reduction. Data reduction was performed after each run, using the standard VTI's T38-APS software package. It was done in several stages, usual for the processing of wind tunnel force tests i.e:

- Reading of raw data-acquisition-system data and signals normalization;
- Determination of flow parameters in the test section of the wind tunnel;
- Determination of model position (orientation) relative to test section and airflow;
- Determination of non-dimensional aerodynamic coefficients of forces and moments.

A parallel-beam 900 mm-dia. schlieren system with three-colour filter and a digital camera was used to create recordings of wind tunnel runs in the test of the 75 mm model. As the purpose of this visualization was primarily the monitoring of the safety of the model [18], only low-resolution recordings (640 × 480 pixels) were made.

DOI: 10.13009/EUCASS2017-213

4.4 Accuracy of measurement

An estimate was made of the accuracy of measurement as the 2σ uncertainty some of the principal quantities on the basis of uncertainties of contributing measurements. Assuming a normal distribution of errors, this interval is, theoretically, supposed to encompass 95% of measurement results. The standard deviation σ_R of a complex measurement in which the resultant quantity R was determined from several independently measured quantities x, y, z,…, each measured with uncertainty $2\sigma_x$, $2\sigma_y$, $2\sigma_z$, …, as:

$$\sigma_R = \sqrt{\left(\sigma_x \frac{\partial R}{\partial x}\right)^2 + \left(\sigma_y \frac{\partial R}{\partial y}\right)^2 + \left(\sigma_z \frac{\partial R}{\partial z}\right)^2 + \ldots} \qquad \textbf{(1)}$$

where the partial derivatives were the "sensitivities" of the determined variable to the changes of the contributing variables.

Because of the difficulty of analytically determining the necessary partial derivatives in the complex calculations needed to obtain the aerodynamic coefficients, the derivations were performed numerically, by varying the data for each directly measured quantity for a small amount (equal to ½ of the nominal uncertainty of each sensor), performing the complete computation of the aerodynamic coefficients, and by noting the changes in the computed output values. Numerical estimates of the partial derivatives were made on the basis of test conditions and values of measured quantities at test Mach numbers, at the angle of attack Alpha of 10º and roll angle Phi of 0º.

Estimated uncertainties of flow parameters shown in Table 2 are independent on the magnitude of measured forces and moments. Therefore, these accuracy estimates can be assumed to be valid for the complete test.

Table 2: Estimated 2σ uncertainty of test conditions

Mach number	**1.5**	**3.0**
2σ M	±0.0007	±0.00055
2σ Po, [bar]	±0.0017	±0.0017
2σ q, [bar]	±0.0007	±0.0004
2σ Re	±3200	±4300
2σ Alpha, [º]	±0.04	±0.04
dPhi, [º]	±0.07	±0.07

Estimated uncertainties of data obtained from the six-component balances are presented in Table 3 and Table 4. The computation is only weakly dependent on the magnitude of measured forces and moments. Therefore, the estimates can be assumed to be valid for all configurations, at any aerodynamic angle. For each Mach number, the balance load ranges and accuracies were taken from the calibration of the balances in the corresponding load range.

Table 3: Estimated 2σ uncertainty of force measurements

Balance	**VTI40B**	**MkXVIII**
Axial force	±0.11%FS	±0.11%FS
Side force	±0.07%FS	±0.15%FS
Normal force	±0.08%FS	±0.17%FS
Rolling moment	±0.17%FS	±0.10%FS
Pitching moment	±0.08%FS	±0.06%FS
Yawing moment	±0.07%FS	±0.08%FS

Table 4: Estimated 2σ uncertainty of aerodynamic coefficients

Model size **Mach number** **Balance**	**75 mm** **1.5** **VTI40B**	**75 mm** **1.5** **MkXVIII**	**75 mm** **3.0** **MkXVIII**	**100 mm** **1.5** **MkXVIII**	**100 mm** **3.0** **MkXVIII**
2σ CA	±0.0029	±0.0068	±0.0058	±0.0040	±0.0033
2σ CN	±0.009	±0.042	±0.036	±0.023	±0.020
2σ Cm	±0.013	±0.054	±0.047	±0.023	±0.020
2σ CAb	±0.0008	±0.0008	±0.0021	±0.0008	±0.0021

4.5 Results and discussion

Available test data on the HB standard models [19], [20]-[26] were examined to establish reference characteristics for the correlation of the T-38 experimental results with those from other aerodynamic facilities, [28]. As reference data at high-AoA was not available, current T-38 results were compared with reference data from the AEDC Von Karman Facility [19][20] and ONERA Chalais, France [21] only in the lower AoA range and in spite of much lower Reynolds numbers in reference tests, ranging from 0.1 to 2.7 millions vs. 2.2 to 4.5 millions in T-38 tests. Comparable high-Reynolds-number reference data could not be found. Other, newer, publications have shown that the HB configurations have recently been used mostly for pressure-distribution and heat-transfer tests, [23]-[26] and force data were not available. Test results were also compared with those from earlier tests [27] of the same 75 mm model in the T-38 wind tunnel in the AoA range up to 15° on a high-drag-range wind tunnel balance designated as BV40. An additional degree of confidence in the high-AoA results was obtained by comparing the results of the T-38 tests with two different model sizes (75 mm and 100 mm forebody diameters).

A good agreement of results in the AoA range common to all tests was observed, the differences between the results and the reference data in most cases being not larger than the differences between the reference data themselves. This is illustrated in Figure 12 and Figure 13 by graphs of test results for the forebody axial force coefficient CAf, total axial force coefficient CA, normal force coefficient CN and pitching moment coefficient Cm, obtained at Mach 1.5 and Mach 3.0, respectively. The agreement of the data for normal force and pitching moment from all sources is particularly good (Figure 12c, Figure 12d, Figure 13c, Figure 13d).

A difference in the character of the total axial force coefficients CA obtained for two model sizes at Mach 1.5 was noted, as well as a difference between the forebody axial force coefficients at AoA above 24° (Figure 12a, Figure 12b). These differences were not observed at any higher Mach numbers. The cause of the differences is, for the time being, unresolved, because the tight test schedule did not permit a repetition of runs in order to gather additional data. As the forebody coefficients agreed well except at the highest AoA, the difference seemed to be related to base drag. The only factors differing between the tests were model size (i.e. Reynolds number) and sting/base diameter ratio. This issue will be investigated further in future tests.

The forebody axial force coefficient CAf was reported in reference AEDC tests [20] as decreasing with angle of attack at Mach numbers below 3 and increasing with angle of attack at Mach numbers above 3 and as being more-less constant with angle of attack at Mach 3. However, in VTI T-38 tests, the forebody axial force coefficient at Mach 3 slightly increased with angle of attack while, at lower Mach numbers, it decreased with angle of attack. Therefore, the change of character of the variation of CAf in VTI's T-38 tests seemed to occur at Mach number slightly below 3, while in AEDC tests it occurred at Mach numbers slightly above 3. Comparable data from ONERA S5 Chalais wind tunnel, though only in limited AoA range, seemed to be in better agreement with VTI T-38 results than with AEDC results (Figure 13a).

Comparison of the measured total axial force coefficient CA with AEDC reference data could not be performed because available AEDC results [20] contain only the forebody axial force coefficient and the base drag coefficient is given only for zero lift. Besides, when those two are added to compute the total zero-lift axial force coefficient, the obtained values differ significantly from those obtained in VTI T-38, ONERA and other laboratories [27][28]. The reason for this discrepancy is unknown.

All aerodynamic coefficients at high angles of attack, except for the axial force coefficient at Mach 1.5, follow the trends set at angles of attack of about 17° - 20° in an almost linear fashion. (Figure 12, Figure 13). This character seems to be similar to that observed in the high-AoA Mach 10 data from JAXA [24].

DOI: 10.13009/EUCASS2017-213

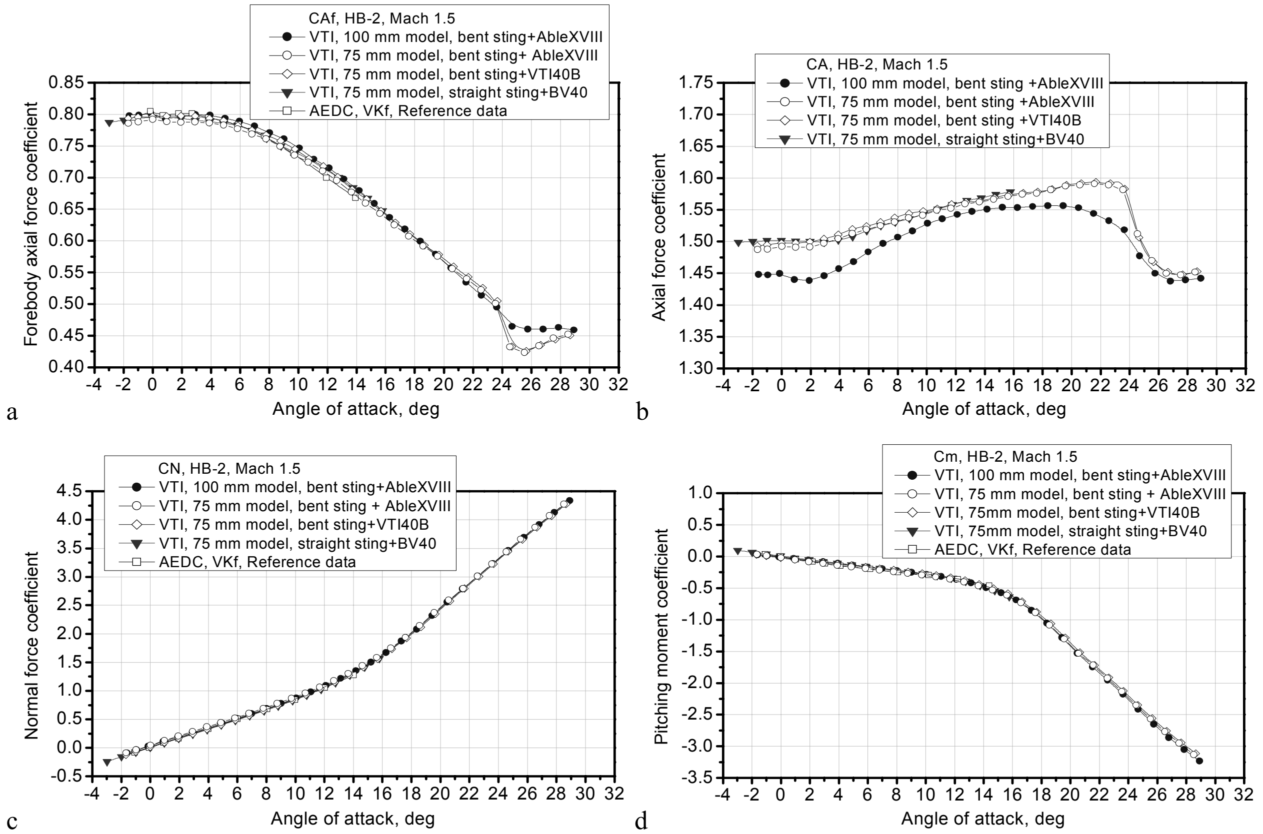

Figure 12: Correlations of the aerodynamic characteristics of the HB-2 model at Mach 1.5

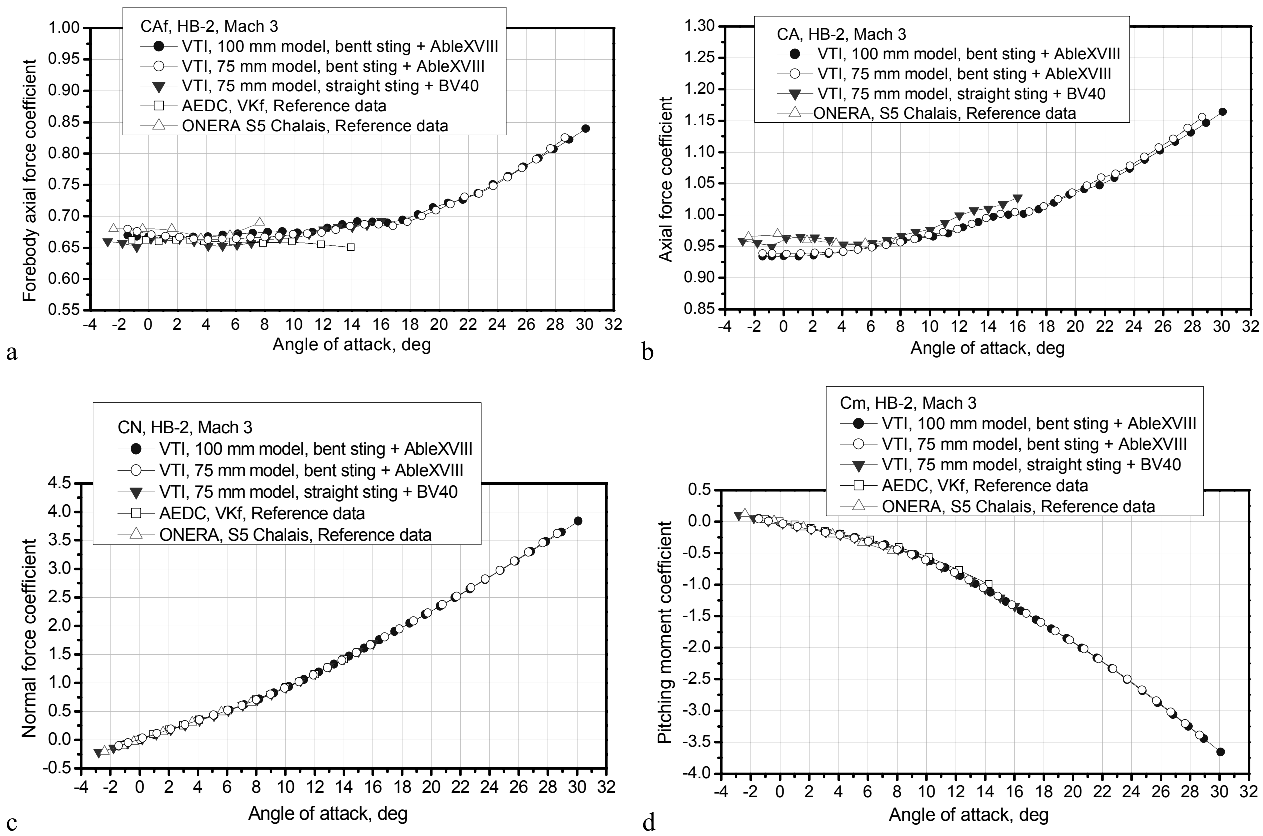

Figure 13: Correlations of the aerodynamic characteristics of the HB-2 model at Mach 3.0

DOI: 10.13009/EUCASS2017-213

Flow patterns around the 75 mm HB-2 model at Mach numbers 1.5, 2.5 and 4 at high angles of attack in the T-38 wind tunnel are illustrated by snapshots of schlieren visualisations shown in Figure 14. When viewing these images one should have in mind that schlieren technique shows the effects of density gradients integrated through the width of the test section, not a “cross-section” of the flow field in the model’s plane of symmetry.


a

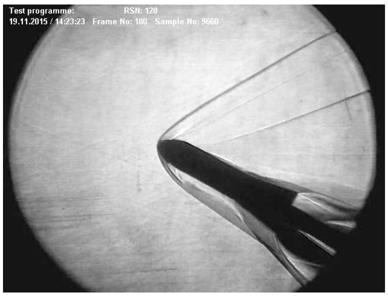
b


c

Figure 14: Snapshots from schlieren-visualization video monitoring of tests of the 75 mm HB-2 model; Mach 1.5, Alpha 29º (a), Mach 2.5, Alpha 30º (b), Mach 4.0, Alpha 22º (c)

5 Conclusions

Responding to a need for standard model data at high angles of attack in the supersonic speed range, a series of tests of two HB-2 models of different sizes were performed in the T-38 wind tunnel of VTI, in Mach number range 1.5 to 4 at angles of attack up to 30° and at relatively high Reynolds numbers of 2.2 millions to 4.5 millions (based on model forebody diameter).

As there were no comparable data at high angles of attack from tests in other facilities, obtained results were compared with references only in the lower angle-of-attack range (up to 15°). Very good correlation was found and, in the absence of any directly comparable reference data at high angles of attack, it is assumed that the obtained results, found to be good at angles of attack up to 15°, are, by implication, also good at higher angles of attack.

The collected data are included in the local database of test results for the HB-2 models that is being formed in VTI, to be used in future periodic verifications of the T-38 wind tunnel in the supersonic part of the operating envelope.

There are indications that there is an observable influence of model size and/or base/sting diameters ratio on the base drag and, therefore, axial force coefficients at Mach 1.5. This is to be investigated in future tests of the same models which will be continued periodically, as circumstances and wind tunnel schedules permit. It is also intended to extend the AoA range up to 40º and to collect some data in the transonic speed range as well.

The results of the performed tests of the HB-2 models will be made available to the wind tunnel community, and they may be found to be of use to the experimenters in other wind tunnel facilities, and as test cases for the high-angle-of-attack CFD codes.

References

[1] Dahlem, V., Flehaerty, J.I., Shereda, D.E. and Prziembel, C.E.G. 1980. High Angle of Attack Missile Aerodynamics at Mach Numbers 0.3 to 1.5, AFWAL-TR-80-3070, Flight Dynamics Laboratory, Wright Patterson Air Force Base

[2] Oberkampf, W.L. and Nicolaides, J.D. 1971. Aerodynamics of Finned Missiles at High Angles of Attack, *AIAA Journal* 9(12): pp. 2378-2384

[3] Anon. 1982. High Angle-of-Attack Aerodynamics, AGARD/VKI Lecture Series 121, AGARD

[4] Hale, W. (ed.). 2010. *Wings in Orbit – Scientific and Engineering Legacies of the Space Shuttle*, NASA, Chap. 4d, pp. 225-241

[5] Stengel, R.F. 1973. Strategies for Control of the Space Shuttle Transition, *Journal of Spacecraft and Rockets* 10 (1): pp.73-84

[6] Rom, J. 1992. *Hign Angle of Attack Aerodynamics: Subsonic, Transonic and Supersonic Flows*, Springer-Verlag, New York

[7] Wood, R.M., Wilcox, F.J., Bauer, S.X.S and Allen, J.M. 2003. Vortex Flows at Supersonic Speeds, NASA TP/2003-211950, NASA Langley Research Center

DOI: 10.13009/EUCASS2017-213

[8] Oyama, A., Ito, M., Imai, G., Tsutsumi, S., Amitani, N. and Fujii, K. 2008. Mach Number Effects on Flowfield over a Delta Wing in Supersonic Region, *46th AIAA Aerospace Meeting and Exhibit*, AIAA-2008-354
[9] Lesieutre, D., Love, J. and Dillenius, M. 1996. High Angle of Attack Missile Aerodynamics Including Rotational Rates – Program M3HAX. In: *Atmospherics Flight Mechanics Conference*, AIAA 96-3392
[10] Chenyan, B., Ziniu, W. 2016. Hypersonic starting flow at high angle of attack, *Chinese Journal of Aeronautics*, 29(2): pp. 297-304
[11] Votta, R. 2008. Advanced Models for Prediction of High Altitude Aero-Thermal Loads of a Space Re-Entry Vehicle, PhD Thesis, Universita degli Studi della Basilicata
[12] Cummings, R.M., Forsythe, J.R., Morton, S.A. and Squires, K.D. 2003. Computational challenges in high angle of attack flow prediction, *Progress in Aerospace Sciences*, Vol.39 No.5, pp. 369-383
[13] Elfstrom, G.M., and Medved, B. 1986. The Yugoslav 1.5m Trisonic Blowdown Wind Tunnel. In: *14th AIAA Aerodynamic Testing Conference*. AIAA 86-0746-CP.
[14] Elfstrom, G.M., and Templin, J.T. 2001. A Canadian Partnership in Development of Aerospace and Automotive Test Technology. *Canadian Aeronautics and Space Journal*. 47(3):1-5.
[15] Damljanović, D., and Rašuo, B. 2010. Testing of Calibration Models in Order to Certify the Overall Reliability of the Trisonic Blowdown Wind Tunnel of VTI. *FME Transactions*. 38(4):167-172.
[16] Damljanović, D., Rašuo, B., and Isaković, J. 2013. T-38 Wind Tunnel Data Quality Assurance Based on Testing of a Standard Model. *Journal of Aircraft*. 50(4):1141-1149.
[17] Vuković, Dj. 1994. Investigation of Supersonic Transient Starting Loads in the T-38 1.5 m x 1.5 m Trisonic Wind Tunnel at Zarkovo. In: *19th Congress of the International Council of the Aeronautical Sciences (ICAS)*. 162-171.
[18] Vuković, Dj., Ćurčić, D., Marinkovski, D., Damljanović, D., Samardžić, M., and Vitić, A. 2014. Living with Supersonic Starting Loads in the T-38 Trisonic Wind Tunnel of VTI. In: *29th Congress of the International Council of the Aeronautical Sciences (ICAS)*. Paper ID_0138.
[19] Gray, J.D. 1964. Summary Report on Aerodynamic characteristics of standard models HB-1 and HB-2. AEDC-TDR-64-137. Arnold Engineering Development Center.
[20] Gray, J.D., and Lindsay, E.E. 1963. Force Tests of Standard Hypervelocity Ballistic Models HB-1 and HB-2 at Mach 1.5 to 10. AEDC-TDR-63-137. Arnold Engineering Development Center.
[21] Ceresuela, R. 1964. Mesurés d'Efforts et de Pressions sur la Maquette Balistique Etalon HB-2 de Mach 2 a Mach 16,5. Note Technique 13/1879 A. ONERA.
[22] Malcolm G.N., Chapman G.T. 1968. A Computer Program for Systematically Analyzing Free-Flight Data to Determine the Aerodynamics of Axisymmetric Bodies. NASA TN D-4766, NASA - Ames Research Center
[23] Kharitonov, A.M., Zvegintsev, V.I., Adamov, N.P, Vasenev, L.G., Kuraeva, A.D., Nalivajchenko, D.G., Novikov, A.V., Shpak, S.I., and Chirkashenko, V.F. 2005. Calibration Trials of Working Capabilities of the New Hypersonic Wind Tunnel AT-303 at ITAM. In: *1st European Conference for Aerospace Sciences (EUCASS)*.
[24] Kuchi-Ishi, S., Watanabe, S., Nagai, S., Tsuda, S., Koyama, T., Hirabayashi, N., Sekine, S., and Hozumi, K. 2005. Comparative Force/Heat Flux Measurements between JAXA Hypersonic Test Facilities Using Standard Model HB-2 (Part 1: 1.27m Hypersonic Wind Tunnel Results). JAXA-RR-04-035E. Japan Aerospace Exploration Agency.
[25] Kuchi-Ishi, S., Watanabe, S., Ueda, S., Tanno, H., Komuro, T., Sato, K., and Itoh, K. 2006. Comparative Force/Heat Flux Measurements between JAXA Hypersonic Test Facilities Using Standard Model HB-2 (Part 2: High Enthalpy Shock Tunnel Results). JAXA-RR-05-030E. Japan Aerospace Exploration Agency.
[26] Tsuda, S., and Watari, M. 2006. Force Tests of HB-2 Standard Model with a New Support System in the JAXA 0.44m Hypersonic Shock Tunnel (HST). JAXA-SP-05-019. Japan Aerospace Exploration Agency.
[27] Vuković Dj., and Damljanović, D. 2015. Evaluation of a Force Balance with Semiconductor Strain Gauges in Wind Tunnel Tests of the HB-2 Standard Model. *Proceedings of the Institution of Mechanical Engineers, Part G: Journal of Aerospace Engineering*. 229(12):2272-2281.
[28] Damljanović, D., Rašuo, B., Vuković, Dj., Mandić, S., and Isaković, J. 2016. Hypervelocity Ballistic Reference Models as Experimental Supersonic Test Cases. *Aerospace Science and Technology*. 52:189–197.
[29] Anastasijević, Z., Samardžić, M., Marinkovski, D., Vrtlar, S. and Rodić, M. 2009. Determination of the T-38 Wind Tunnel Oscillatory Data of the Dynamic Missile Calibration Model. *Scientific Technical Review*. 59(2):24-29.
[30] Damljanović, D. 2014. Measurement Accuracy of Flow Field Parameters in Supersonic Wind Tunnels. PhD Thesis. University of Belgrade, Faculty of Mechanical Engineering.
[31] Damljanović, D., and Vuković, Dj. 2016. Selection Criteria of Optimal Conditions for Supersonic Tests in a Blowdown Wind Tunnel. *Scientific Technical Review*. 66(1):29-39.